2004 International Symposium on Nonlinear
Theory and its Applications (NOLTA2004)
Fukuoka, Japan, Nov. 29 - Dec. 3, 2004

Real-time classification methods for biological tissues

Nicola Testoni, Luca De Marchi, Nicolò Speciale, Guido Masetti

DEIS University of Bologna
Viale Risorgimento 2, 40136, Bologna, Italy
email:ntestoni@deis.unibo.it

Abstract—Echographic equipments generate images from almost any kind of soft tissues and allow for diagnosis methods that are receiving increasing attention in modern medical procedures for their non invasive features. For such an instrumentation, real-time processing becomes every days more important; thus, techniques for the elimination of redundancies, bottlenecks and recalibration of configuration parameters for performance optimization are mandatory. In this work we highlight the main issues for real-time performances; in addition, we describe a new optimized method with a threshold detection algorithm. Finally, some results from *in-vivo* and *in-vitro* analysis are discussed.

1. Introduction

Echographic signals result from the interaction between the pressure wave generated by the transducer and the tissue structure. Let $h(t)$ be the ultrasound pulse shape and $s(t)$ be the scatter distribution. Under the assumptions of weak scattering, narrow ultrasound beam and linear propagation, the echo signal $y(t)$ can be expressed [1] as

$$y(t) = s(t) * h(t) = c(t) + d(t) = \sum_{n=1}^{N_c} c_n(t-\theta_n) * h(t) + \sum_{n=1}^{N_d} d_n(t-\tau_n) * h(t) \quad (1)$$

where $c(t)$ derives from the interaction of the pulse with the resolvable scatterers, $d(t)$ with the randomly located diffuse scatterers, while N_c and N_d are the number of coherent and diffuse scatterers, θ_n and τ_n their time delays to the receiver, and c_n and d_n their relative strengths. As sampling does not alter superposition, one gets:

$$y(n) = c(n) + d(n) \quad (2)$$

The Wold-decomposition theorem can split $y(n)$ into its two components [2]. The diffuse component $d(n)$ is well modeled by an autoregressive (AR) stochastic process. The coherent component $c(n)$ is approximated by a summation of Gaussian modulated sinusoid: the resolvable scattering structure can be viewed as a summation of delta functions of random strength located at the resolvable scatterers' location, while the echo pulse can be approximated by a Gaussian modulated sinusoid.

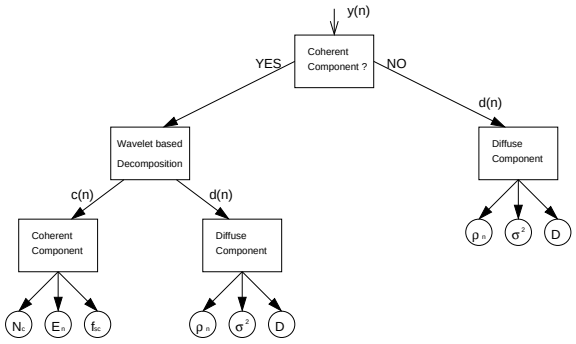

Figure 1: CWTD algorithm diagram

2. Georgiou-Cohen algorithm

As $c(t)$ and $d(t)$ overlap in time and frequency, to separate the two components and extract structural parameters one can adopt the algorithm proposed by Georgiou and Cohen [3] based on the time-frequency properties of the Continuous Wavelet Transform Decomposition (CWTD) (see Fig.1). This algorithm first checks the existence of coherent scatterers testing the hypothesis of Rayleigh scattering by means of the non-parametric Kolmogorov-Smirnov (K-S) test for color field [4]: if this does not hold, i.e. a coherent part exists, the echo signal is decomposed into its two components. After decomposition, the CWTD algorithm estimates the parameters needed to classify the tissue.

2.1. Coherent component detection

The K-S test statistic assumes random samples. Since the echo signal is correlated, data first need to be decolored: this can be achieved by modeling the signal as an AR(p) process, using the fast Burg algorithm [5] to calculate its coefficients, and then extracting the innovation sequence. The K-S statistic D is then calculated by:

$$D = \sup_{-\infty<w<\infty} |P(w) - G(w)| \quad (3)$$

where $G(w)$ is the supposed Gaussian distribution and $P(w)$ is the empirical cumulative distribution function (ECDF) of $w(n)$, defined as:

$$w(n) = y(n) - \sum_{k=1}^{p} a_k y(n-k) \tag{4}$$

where $y(n)$ is the input signal, p is the model order and a_k are the model coefficients.

Burg algorithm cannot be executed on streaming data and it is somewhat burdensome in a real-time environment because of the high number of multiplication and division needed. For the echo signal analysis the Levinson algorithm [5] is a valid alternative.

The extraction of the innovation sequence is not an issue, since it is done through FIR filtering, while statistical testing requires a great use of resources. As the K-S test is based on the ECDF, an histogram estimation routine must be used. These routines usually involve sorting steps thus an high number of comparisons: this means that streaming data can be processed only through buffering.

2.2. Wavelet based decomposition

In presence of a coherent component, the wavelet power fluctuations over J different scales are examined using the Scale-Average wavelet Power spectrum (SAP),

$$\overline{W}^2 = \frac{1}{J} \sum_{j=1}^{J} |W(s_j, n)|^2 \tag{5}$$

where $W(s_j, n)$ are the wavelet coefficients of $y(n)$ at the j-th scale. The detection and time localization of the coherent scatterers are performed by thresholding the SAP with:

$$\theta_{SAP} = \mu_\omega + \theta \sigma_\omega \tag{6}$$

where μ_ω is the SAP mean value, σ_ω is its standard deviation and θ a tuning parameter.

The CWTD algorithm in [3] uses the Morlet wavelet, so very long Wavelet filters and an high number of non trivial multiplication are expected. Since it is important to consider all signal bandwidth in the SAP calculation, a certain number of CWT must be calculated before final summation, increasing the total number of multiplication. Finally, to calculate standard deviation a square root routine is executed. Thresholding is a critical phase in the characterization algorithm, so the square root result should have the same accuracy of the SAP mean value: this could require iterative algorithms with lookup tables.

2.3. Component features extraction

Even if CWTD algorithm in Fig.1 estimates three different features for each component, it was reported in [3] that only two of them can be fruitfully used in a classification process. In particular, the mean energy E_n of the coherent scatterers is most successful in discriminating between normal, fibrocystic, cancer and fibroadenoma tissues, while the residual error variance σ^2 of the diffuse scatterers is able to differentiate between malignant and benignant tissues, such as normal, fibrocystic and fibroadenoma tissues.

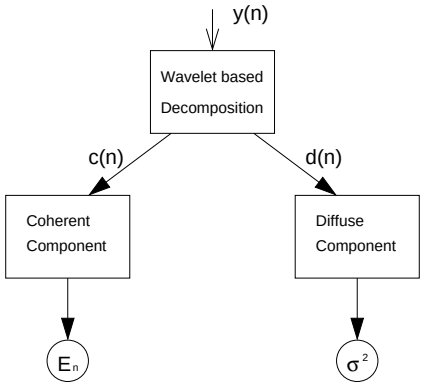

Figure 2: Optimized CWTD algorithm diagram for real-time execution

3. Real-time classification algorithm

The CWTD algorithm can be reworked to achieve real-time processing capabilities. First of all, if we hypothesize that the input signal always contains a coherent and a diffuse component, the detection stage of the former can be eliminated. When this hypothesis is not verified, the decomposition block must generate a zero value coherent signal by using a fixed threshold, which eliminates the necessity of the square root calculation too. The resulting modified algorithm for E_n and σ^2 calculation is shown in Fig.2.

3.1. Components separation

We used the Wavelet Transform (WT) to separate the frequency contents while keeping time information. Since this transform preserve energy, a thresholding operation to eliminate coefficients of the diffuse component is feasible. A good estimate of $c(t)$ is reconstructed by inverse transformation and $d(t)$ is extracted by subtraction from the original signal.

Viewing the WT as a filter stage, the central frequency and the bandwidth can be set freely using a single Wavelet Packet Transform (WPT) [6], while the discrete realization of the CWT needs multiple analysis. Moreover, the structure of the WPT allows for the change of both central frequency and bandwidth at runtime while the filter coefficients remains fixed. We propose to replace the multiple CWT and the SAP calculation with a single WPT followed by an energy

estimation.

Since we aim to cover all the signal bandwidth while maintaining a low computational cost, Haar wavelet which avoids multiplication seems particularly useful: only additions and shifts are used to filter the signal preserving accuracy.

Thresholding has proven most successful when based on mean energy over a fixed length set of samples: whenever energy is lower than threshold, the corresponding wavelet packet coefficients are set to zero. Optimization of this process reduced the operation to a single multiplication and two algebraic sums, while keeping real-time processing capabilities. Finally, the Inverse Wavelet Packet Transform (IWPT) allows us for the reconstruction of the coherent component with low computational cost and high efficiency.

3.2. Components analysis

The residual error variance is estimated from the innovation sequence of the AR(p) diffuse component model. The use of Levinson algorithm reduces the computational cost of whitening coefficient estimation, but it requires an estimation of the input signal autocorrelation function (ACF). This is usually performed through FFT-based algorithms; these techniques, however, are time and resource consuming in a real-time environment, requiring $\max\{N,K\} \times log_2(\max\{N,K\})$ multiplication to estimate the first K terms of the ACF from a sequence of N samples.

A more efficient, real-time capable algorithm can be derived taking care of the time dependence definition of ACF: this algorithm uses only K multiplications to extract the first K terms of the ACF from a sequence of N samples.

Since Levinson algorithm cannot process streaming data, buffering is required. Thus, after ACF estimation, input streaming data are delayed with a shift-register with N_p memory locations while whitening coefficients are estimated. The ACF coefficients are sampled each N_p samples and then used to estimate the new set of whitening coefficients a_k applying the Levinson algorithm. The value of N_p must be set accordingly to the time needed to estimate the new coefficients.

In order to avoid unwanted overwriting during updating, the coefficients are buffered and then used in a the FIR filter to extract the white innovation sequence. Additionally, only one multiplication and a reduced number of algebraic sums are necessary to obtain an unbiased variance estimation

$$\sigma^2 = \sum_{i=1}^{N} \frac{(x_i - \overline{x})^2}{N-1} \tag{7}$$

Finally, estimation of the mean energy E_n of the coherent scatterers is quite simple, as the mean operator is unbiased. We found that E_n can be achieved through one multiplication and two algebraic sums only.

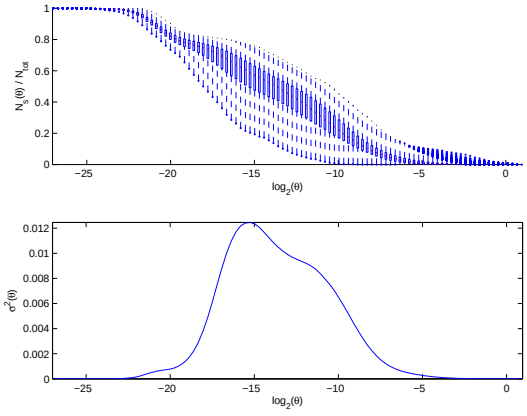

Figure 3: Statistical analysis for echo samples: normalized number of over-threshold samples (top) and variance of over-threshold samples (bottom) versus threshold log_2

4. Threshold detection algorithm

The threshold value must be finely tuned and extracted off-line: as we use a statistical approach, a great number of samples obtained from echographic videos is required.

First, we extract the CDF of the samples mean energy for each acquisition and we calculate the number of samples over a given threshold versus the threshold itself (Fig.3a). These functions have a characteristic behavior; apart the zones at the ends, the slope in the intermediate region depends on the strength of the coherent component compared to the diffuse one: when coherent component is absent, low power samples are predominant and viceversa. This moves the slope from left to right. The statistical distribution of these functions (Fig.3b) shows a single maximum that corresponds to a good thresholding value for the data set.

5. Results

The proposed optimized algorithm has been applied to both *in-vivo* and *in-vitro* echo images. Figg.4-5 show some cases acquired with a LA13 transducer with a central frequency of 7.5 MHz and a bandwidth of 5 MHz at -6 dB.

Resolvable scatterers images (Figg.4-5b) show an improvement in contrast and tissue separation, in particular for *in-vitro* echo images. Thus, the achieved images can be useful in discriminating between normal, fibrocystic, cancer and fibroadenoma tissues.

Diffuse error variance images (Figg.4-5c) show an

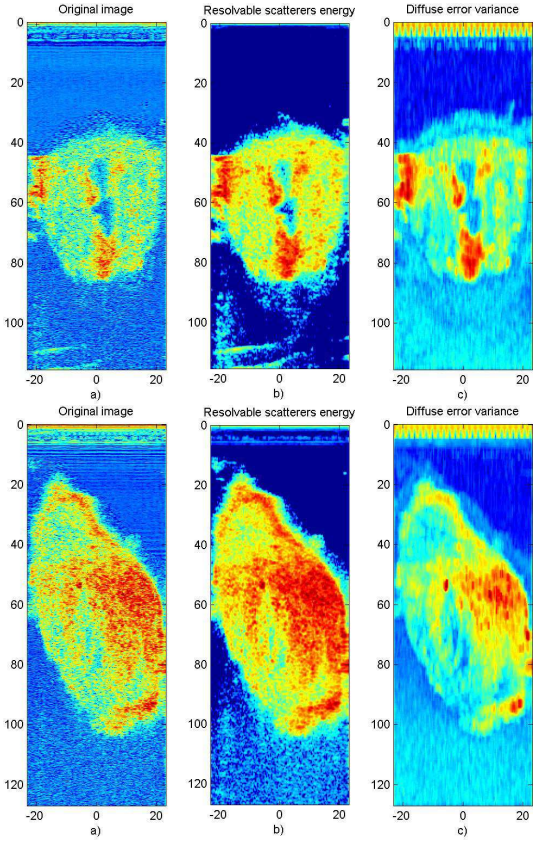

Figure 4: In-vitro prostatic gland affected by carcinoma; from left to right a) originale image, b) resolvable scatterer energy and c) diffuse error variance

improvement in contrast too, even if tissue separation is not as good as in the previous case. However, benignant versus malignant tissue classification is possible by inspecting these images.

6. Conclusions

In this work we have presented an optimized form for the CWTD algorithm for tissue classification suitable for real-time data processing. We showed that a good value for energy thresholding can be obtained from a statistical analysis of echographic video. The proposed algorithm was tested on real ultrasound images and satisfactory visual tissue discrimination was demonstrated.

7. Acknowledgments

The authors gratefully acknowledge Prof. Masotti (University of Florence) and his group for providing *B-Mode* images. This work has been partially supported by MIUR within the framework of Cofin2002 founding initiative.

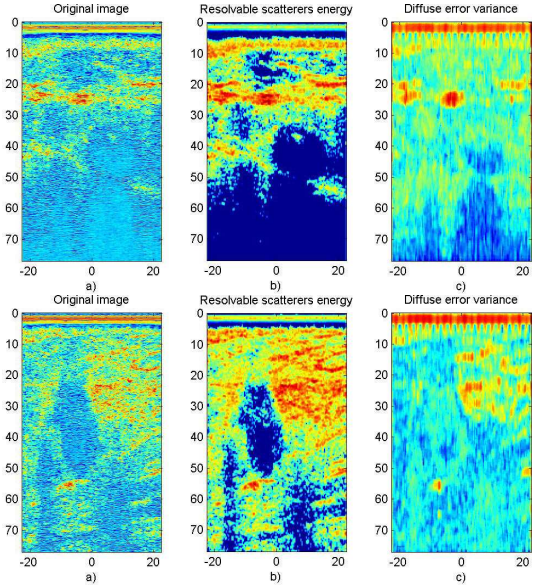

Figure 5: In-vivo breast with sebaceous cyst (top) and adenocarcinoma (bottom); from left to right a) originale image, b) resolvable scatterer energy and c) diffuse error variance

References

[1] M.F. Insana, R.F. Wagner, D.G. Brown, T.J. Hall, "Describing small-scale structure in random media using pulse-echo ultrasound", *J. Acoust. Soc. Amer.*, vol.87, pp.179-192, 1990.

[2] F.S. Cohen, G. Georgiou, E. Halpern, "WOLD decomposition of the backscatter echo in ultrasound images of soft tissue organs", *IEEE Trans. on Ultrason., Ferroelec., freq. Contr.*, vol.44, pp.460-472, 1998.

[3] G.Georgiou, F.S. Cohen, "Tissue Characterization Using the Continuous Wavelet Transform – Part I: Decompostion Method", *IEEE Trans. on Ultrason., Ferroelec., freq. Contr.*, vol.48, no.2, pp.355-363, 2001.

[4] G. Georgiou, F.S. Cohen, "Statistical Charcterization of Diffuse Scatetring in Ultrasound Images", in *IEEE Trans. on Ultrason., Ferroelec., freq. Contr.*, vol.45, no.1, pp.57-64, 1998.

[5] S.M. Kay, "Modern Spectral Estimation", Englewood Cliffs: PTR Prentice Hall, 1988.

[6] R.R. Coifman, Y. Meyer, M.V. Wickerhauser, "Wavelet analysis and signal processing", *Wavelets and their applications*, pp.153-178, Jones and Barlet: B. Ruskai et al. editors, 1992.